NJC

Accepted Manuscript

This is an *Accepted Manuscript*, which has been through the Royal Society of Chemistry peer review process and has been accepted for publication.

Accepted Manuscripts are published online shortly after acceptance, before technical editing, formatting and proof reading. Using this free service, authors can make their results available to the community, in citable form, before we publish the edited article. We will replace this *Accepted Manuscript* with the edited and formatted *Advance Article* as soon as it is available.

You can find more information about *Accepted Manuscripts* in the Information for Authors.

Please note that technical editing may introduce minor changes to the text and/or graphics, which may alter content. The journal's standard Terms & Conditions and the Ethical guidelines still apply. In no event shall the Royal Society of Chemistry be held responsible for any errors or omissions in this *Accepted Manuscript* or any consequences arising from the use of any information it contains.

ROYAL SOCIETY OF CHEMISTRY

www.rsc.org/njc

A study of $Pd^{(0)}$ modified MCM-48 mesoporous microsphere with ultrahigh surface area catalyzed hydrodechlorination of 4-Chlorophenol

*Yansheng Liu, Xinlin Li, Xuanduong Le,Wei Zhang, Hao Gu, Ruiwen Xue and Jiantai Ma**

Gansu Provincial Engineering Laboratory for Chemical Catalysis, College of Chemistry and Chemical Engineering, Lanzhou University, Lanzhou 730000, PR China.

** Corresponding author, E-mail addresses: majiantai@lzu.edu.cn (Jiantai Ma).*

Tel.: +86 0931 891 2577; Fax: +86 0931 891 2582

Abstract

MCM-48 mesoporous microspheres (M48N) with pore size of 3.77 nm, ultrahigh surface area of 1250.77 m^2 g^{-1} and super-large pore volume of 1.52 cm^3 g^{-1} has been synthesised. Pd, Pt and Ru nanoparticles (NPs) modified M48N were prepared by incipient wetness impregnation and had been investigated for hydrodechlorination (HDC) in aqueous phase using 4-chlorophenol as target compound. The catalysts Pd, Pt, Ru/M48N were characterized by transmission electron microscope, X-ray diffraction, nitrogen adsorption–desorption and X-ray photoelectron spectroscopy measurements. The HDC experiments were performed at room temperature and atmospheric H_2 pressure, fairly mild conditions for a potential application to treat industrial wastewater. By analysing the catalytic results, Pd/M48N exhibited higher catalytic performance than Pt, Ru/M48N and some other kind of Pd based catalysts. The high catalytic performance of Pd/M48N owing to ultrahigh surface area, super-large pore volume and unique pore structure of the M48N which can improve mass transfer and increase adsorption–desorption rate of compounds.

Keywords**:** MCM-48 mesoporous microsphere, metal nanoparticles, HDC reaction, 4-chlorophenol

1. Introduction

In recent years, environmental problems have attracted much attention. One of these environmental issues is the pollution caused by synthetic industrial organic waste. 4-Chlorophenol (4-CP) as an important commercial product has been broadly employed as the raw material for the preparation of herbicide, production of pesticides and disinfectors.[1, 2] Huge amounts of applications of 4-CP have resulted in un-ignorable environmental problems because of its persistent toxic and the degradation-resistant. Therefore, how to deal with the pollution caused by 4-CP has become an important issue which has attracted a lot of researchers. Till now, many reported traditional methods including thermal combustion, reduction dechlorination,[3, 4] oxidation dechlorination,[5] biodegradation and photocatalytic degradation, have been employed to dispose the wastewater containing 4-CP. Although there were some advantages, it cannot be ignored that these kinds of methods cannot completely decompose 4-CP into simple inorganic compound such as CO_2, H_2O and HCl. On the contrary, toxic chlorinated chemicals such as dioxins, phosgene and chlorine can be formed in the process of these treatments of 4-CP.[6] These accompanied chemicals can result in secondary pollution and especially did harm to the health of human beings and atmospheric ecosystem. Compared with traditional treatments of 4-CP mentioned above, hydrodechlorination (HDC) had attracted much attention. By using efficient catalysts, the reaction can be performed under a mild condition and energy consumption can be reduced. In addition, it can reduce the formation of by-product

and can be suitable for the treatment of a wide range of chlorinated compounds.[7] In the consideration of economic and environmental points, catalytic HDC had been considered as an effective and promising method.

The liquid phase catalytic HDC had been reported by many groups.[7-9] The studies in the literature mainly focus on the catalytic activities which affected by active phase, support, sources of hydrogen, or reaction media.[10, 11] So far, a large number of catalysts using metal NPs as active sites had been developed for HDC of 4-CP, such as supported Pd[11-15], Pt[16, 17], Rh[18] and Ni.[15] Among them, supported Pd catalysts showed an excellent catalytic activity for the treatment of 4-CP. According to the experimental results which had been reported, it agreed that small NPs can provide higher catalytic activity, which mostly contributed to surface atoms residing on the edges of the crystallographic planes or on edge junctions. These atoms increased the numbers of active sites which could be accessible to the 4-CP molecules.[7, 19, 20] According to studies of L. Calvo[21] and F. J. Urbano1,[19] it seems that HDC was structure-sensitive reaction. So, the effects of supports in HDC reactions had been extensively studied. Many supports, such as activated carbon,[22-24] Al_2O_3[25] or zeolites[26, 27] had been employed to prepare catalysts for HDC of 4-CP. Recently, Chia-Min Yang reported a synthesis of MCM-48 mesoporous microsphere (M48N).[28] As support, M48N possessed some excellent characters such as pore size of 3.77 nm, ultrahigh surface area of 1250.77 $m^2 g^{-1}$ and super-large pore volume of 1.52 $cm^3 g^{-1}$. The ultrahigh surface area can provide much external surface to load more metal NPs.

The channel structure also can provide internal surface area and active sites. Besides, ultrahigh surface area can make the loaded metal NPs disperse well-distributed. The well-dispersed metal NPs on support can make reactant molecules combine to active sites more easily and make product molecules desorb from active sites more quickly so that the reaction rate can be raised. These particular characters cannot be found in some other catalysts with low surface areas and non-channel structure.

Based on the above considerations, in this study, we chose Pd, Pt and Ru NPs as the active phase and M48N as support to prepare supported metal nanocatalysts, and their catalytic performance for HDC of 4-CP had also been studied.

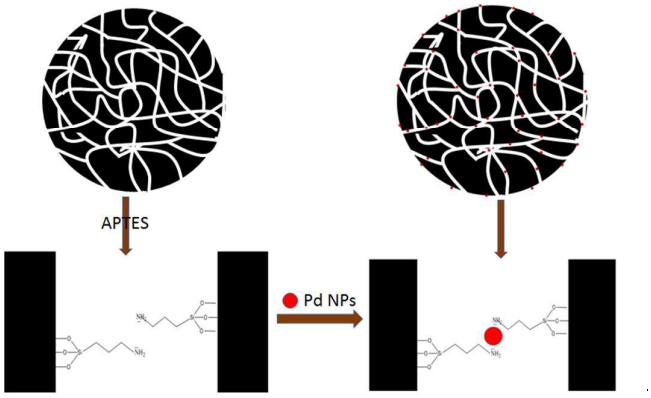

Scheme 1. Preparation of Pd/M48N nanocatalyst.

2. Experimental

2.1 Materials

Tetraethoxysilane (TOES), Pd(II) acetate, chloroplatinic acid , ruthenium chloride, Benzylcetyldimethylammonium chloride (BCDAC) and (3-aminopropyl)triethoxysilane (APTES) were purchased from Aladdin Chemical Co., Ltd. 2-chlorophenol (2-CP), 3-chlorophenol (3-CP), 4-chlorophenol (4-CP),

2,4-dichlorophenol (2,4-DCP) and 2,4,6-trichlorophenol (2,4,6-TCP) were purchased from Lanzhou Aihua Chemical Company. $NaBH_4$ was supplied by Sinophrm Chemical Reagent Co., Ltd. Organic solvents used were of analytical grade and did not require further purification.

2.2 Preparation of Pd, Pt, Ru/M48N catalysts

M48N was prepared according to the procedure reported by Chia-Min Yang.[28] In this work, a simple and green method (Scheme 1) has been used to prepare the Pd, Pt, Ru/M48N catalysts. Firstly, M48N was functionalized with APTES to obtain M48N-NH_2 nano-composites. Secondly, 500 mg of M48N-NH_2 nanocomposite were added in a 100 mL round-bottom flask with 54 mg of $Pd(OAc)_2$ and 50 mL of acetonitrile, then ultrasonically dispersed for 30 min and keep stirring for 12 h. Subsequently, the fresh $NaBH_4$ solution (0.2 M, 20 mL) was added dropwise into the abovementioned suspension. The product was isolated by centrifugation and washed several times with deionized water and ethanol, and then dried in a vacuum overnight. The Pt/M48N and Ru/M48N were prepared through the same method.

The metal loading of Pd, Pt and Ru were 5.01%, 4.72 and 5.05% which were measured by ICP measurement.

2.3 General procedure for the HDC of 4-CP.

HDC experiments were performed in a 50 mL three-necked jacketed glass reactor equipped with H_2 supplied. 20 mg of catalyst was placed into mixed solution of 30 mL solvent, 1 mmol of CPs and a certain amount of base under H_2 continuously

passed at 30 mL min^{-1}. The reaction maintained for 2 h under vigorous stirring at 20 °C. The results of the experiments were analysed by Gas Chromatography (GC).

2.4 General methods

Transmission electron microscopy (TEM) images were obtained on a Tecnai G2 F30, FEI, USA. The Brunauer–Emmett–Teller (BET) surface area and pore-size distribution were obtained by measuring N_2 adsorption isotherms at 77 K using a TriStar 3020 (Micromeritics). Powder x-ray diffraction (XRD) spectra were obtained by a Rigaku D/max-2400 diffractometer using Cu-Kα radiation in the 2θ range of 0.5°-80°. X-ray photoelectron spectroscopy (XPS) was recorded on a PHI-5702 and the C1S peak at 284.6 eV was used as the binding energy reference. The reaction conversion was estimated using GC (P.E. AutoSystem XL).

3. Results and Discussion

In this study, the catalyst activity of M/M48N was tested using CPs as target compound under different condition and glass flask supplied with H_2 was used as reaction reactor.

3.1 Characterization

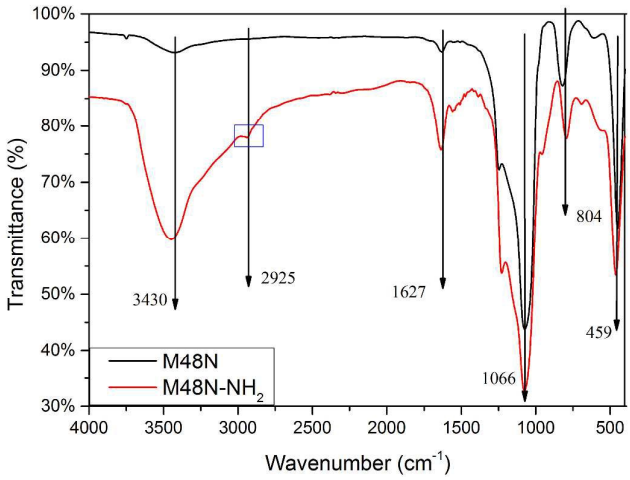

Figure1. FT-IR spectra of M48N and M48N -NH_2.

Figure 1 shows the FT-IR spectra of M48N and M48N-NH_2. The adsorption peaks at 1066 cm^{-1} and 804 cm^{-1} corresponding to the antisymmetric and symmetric stretching vibrations of Si–O–Si bond in oxygen-silica tetrahedron, respectively. The peak at 459 corresponds to Si–O stretching. The strong peak at 3430 cm^{-1} shows a large number of Si–OH groups proved to be advantageous to the modification of APTES on the M48N surface by hydrogen bonds. The adsorption peak at 2925 cm^{-1} corresponds to -CH stretching. In the FT-IR spectrum of M48N-NH_2, the peak around 3430 cm^{-1} represents the adsorption of –OH and –NH_2 groups. The nitrogen, hydrogen, and carbon contents of M48N were 0.0%, 0.70%, and 0.267% and the nitrogen, hydrogen, and carbon contents of M48N-NH_2 were 2.37%, 9.02 %, and 2.452%, measured by the elementary analysis, respectively. The FT-IR spectra and elementary analysis result reveal that the APTES is successfully grafted on the M48N surface, thus enabling them to act as robust anchors for metal NPs.

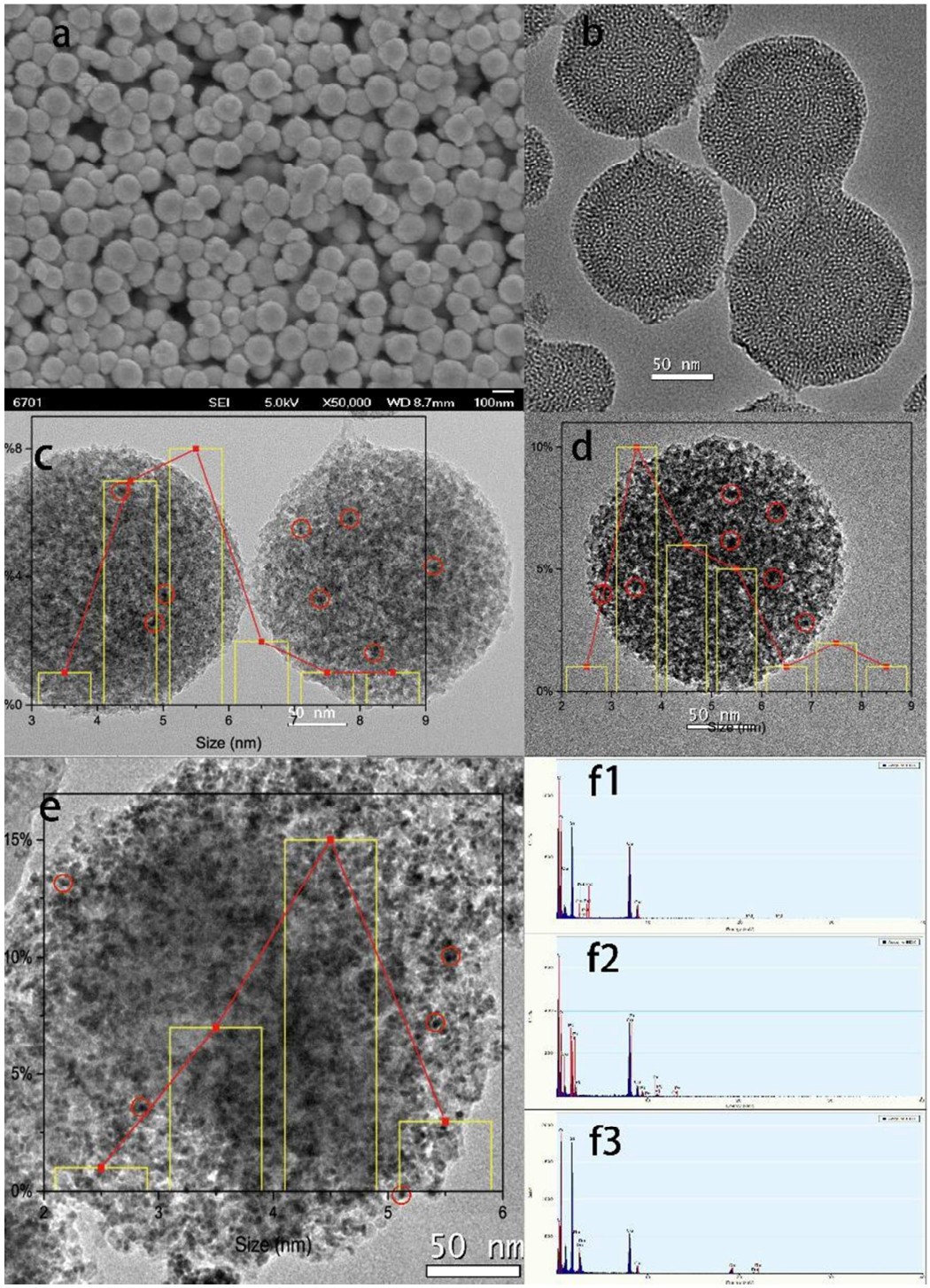

Figure 2. SEM image of M48N(a) and EDX Spectroscopy and TEM images of M48N (b), Pd/M48N (c, f2), Pt/M48N (d, f2), Ru/M48N (e, f3).

TEM images of M48N and Pd, Pt, Ru/M48N were shown in Figure 2. M48N

particles with diameter of ~200 nm and sphere structure were exhibited in Figure 2a and Figure 2b. From TEM image of M48N, it indicated that all channels in M48N seemed connected. EDX Spectroscopies of as-prepared samples were exhibited in Figure f which suggested the metal NPs were loaded in M48N. The TEM images of Pd, Pt and Ru loaded on M48N were displayed in Figure 2c, 2d and 2e, respectively. Also size distribution of M/M48N has been made, and the main size of Pd, Pt and Ru NPs range between 3-6 nm. From each M/M48N, it can be seen that the noble metal NPs loaded on both surface and pore surface of M48N and this caused the difference of TEM images of M48N and M/M48N.

Table 1. The surface area, pore volume, pore size of M48N and Pd, Pt, Ru/M48N.

Samples	Surface Area (m^2/g)	Pore Volume (cm^3/g)	Pore Size (nm)
M48N	1250.77	1.523	3.772
Pd/M48N	1126.65	0.977	3.036
Pt/M48N	1230.33	1.225	3.201
Ru/M48N	1219.27	1.123	2.776

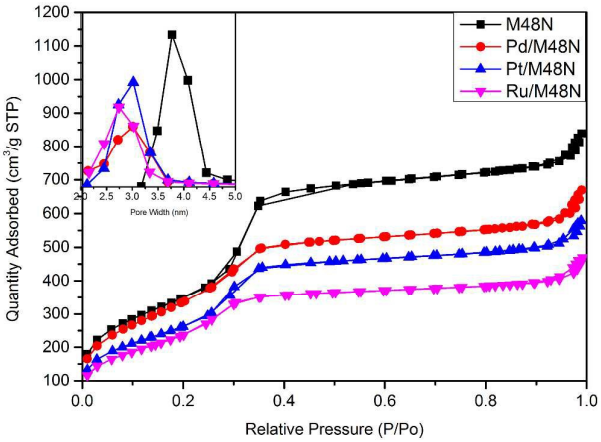

Figure 3. Nitrogen adsorption–desorption isotherms and pore size distribution (*inset*) of M48N and Pd, Pt, Ru/M48N.

N_2 adsorption-desorption isotherms for the M48N and as-prepared samples were given in Figure 3. According to the IUPAC classification, the curves of M48N and all samples were type IV isotherms with a very sharp capillary condensation step at P/P_0 = 0.25–0.40 and H_2-type hysteresis loop characterizing small-pore mesoporous materials with cylindrical channels. The pore size of M48N derived from the BJH analysis on the desorption branch was 3.77 nm. The calculated BET surface area and pore volume of M48N were 1250.77 $m^2 g^{-1}$ and 1.52 $cm^3 g^{-1}$, respectively. Compared with M48N, the pore size of all samples reduced from 3.77 nm to ~3.0 nm and the pore volume values reduced from 1.52 $cm^3 g^{-1}$ to ~1.1 $cm^3 g^{-1}$ which owing to the channels dispersed by metal NPs. Besides, surface area of as-prepared samples maintained at the level of ~1200 $m^2 g^{-1}$ (Table 1).

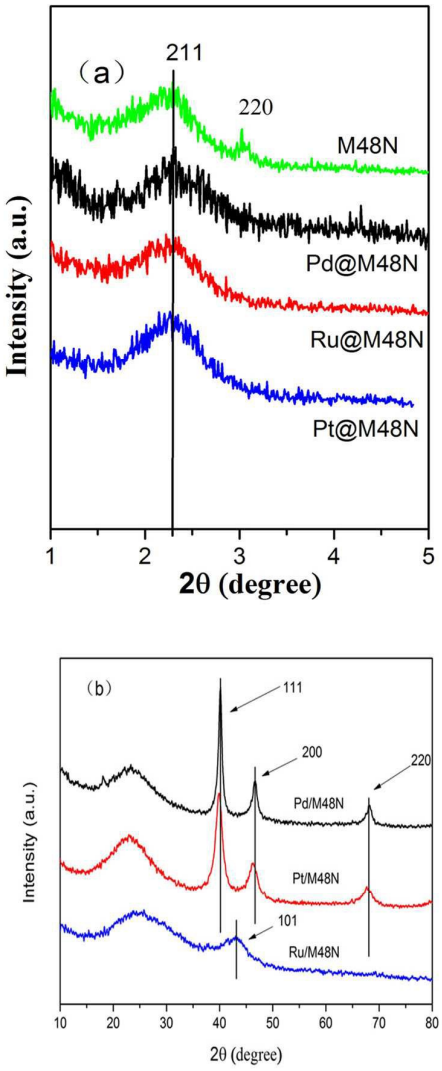

Figure 4. Small-angle (a) and Wide-angle (b) XRD patterns of M48N and Pd, Pt, Ru/M48N.

The small-angle and wide-angle XRD patterns of M48N and the as-prepared samples were given in Figure 4. Frome Figure 4, there were two peaks belong to M48N which correspond to plane (211) and (220) can be observed. One major diffraction peak of metal NPs modified M48N was observed. By comparing with M48N, this difference may be caused by the NPs which load in pore of M48N and resulted in the structure degeneration of M48N. Combined with TEM images and nitrogen adsorption–desorption isotherms, it indicated the mesopore structure of

M48N. From the Figure 4b, Pd/M48N and Pt/M48N possessed three peaks corresponding to planes (111), (200), (220) of Pd and Pt NPs. Ru/M48N possessed one peak corresponds to plane (101) which belonged to Ru NPs.

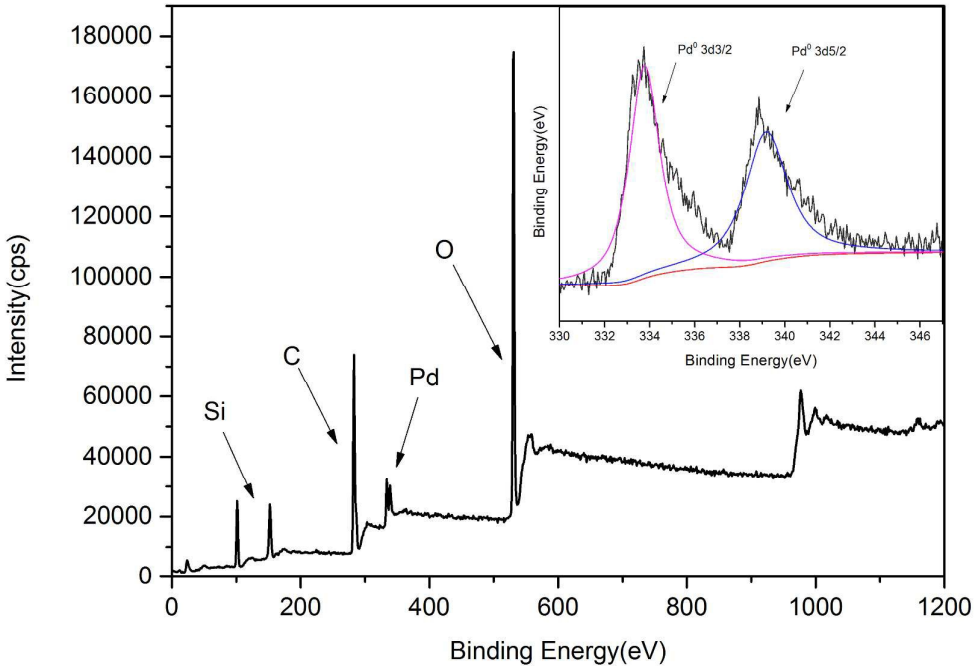

Figure 5. XPS spectra of Pd/M48N (*inset image: high resolution spectrum of Pd 3d*).

The electronic state of the Pd species on the M48N was measured with the XPS. The pattern of Pd/M48N catalyst was exhibited in Figure 5. The Pd 3d peaks in XPS spectra showed that the binding energy values at 334.7 eV and 340.3 eV, which were attributed to the $3d_{5/2}$ and $3d_{3/2}$ peaks of Pd 3d. In addition, no evidence proved the presence of palladium oxide which indicates $Pd(OAc)_2$ was completely reduced to Pd NPs.

3.2 HDC of 4-CP

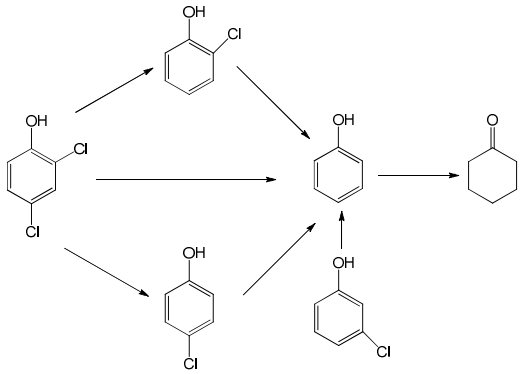

Scheme 2. Schematic of the HDC pathway for CPs.

The catalytic activity of the M48N nanocatalyst was established by the HDC of 4-CP under a mild condition. The HDC of 4-CP was negligible without catalyst or in the presence of pure M48N at the same conditions, which shows that the presence of noble metal NPs were indispensable for high catalytic activity. The HDC pathway is shown in scheme 2. As Diaz et al.[16] explained in a previous work the route of 4-CP HDC proceeded through a set of series-parallel reactions where 4-CP gives rise to phenol and cyclohexanone (CYC) being this last also produced from phenol hydrogenation. Compared with the reactant 4-CP, the two products detected are low toxic and useful as intermediates in production of high value-added chemicals. In this work, the high selectivity product phenol was observed. The low selectivity of HDC of 4-CP performed in fixed bed reactor[29, 30]or under a high H_2 pressure condition,[16] such as: Pd/C catalyzed HDC of 4-CP with the conversion of 93% and the selectivity of 85% were reported by L. Calvo which formic acid as hydrogen source in continuous stirred-tank reactor.[31] Pd/Al_2O_3 as HDC catalyst were also studied by E.

Diaz.[29] in fixed bed reactor with the conversion was 87% and the selectivity 62%, respectively. Compared with reports above mentioned, in our reaction, a batch stirred tank reactor was used and only H_2 was flowing phase. The main production was phenol and less than 0.1% CYC was detected after 120 min reaction time. These differences may be caused by the using of different reaction systems. This result was agreed with the study using same reaction system which phenol as major product was detected.[32-36]

Table 2. The yield of HDC of 4-CP catalyzed by Pd, Pt, Ru/M48N in different reaction conditions.

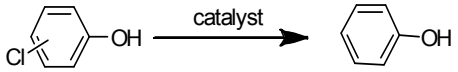

Reactant	Catalyst	Base	Solvent	Yield %
4-CP	[a]Pd/M48N	Na_2CO_3	H_2O	83.6%
4-CP	[a]Pd/M48N	NaAc	H_2O	64.2%
4-CP	[a]Pd/M48N	triethyl amine	H_2O	47.4%
4-CP	[a]Pd/M48N	NaOH	ethyl acetate	1.4%
4-CP	[a]Pd/M48N	NaOH	ethyl alcohol	0.6%
4-CP	[a]Pd/M48N	NaOH	H_2O	99.1%
4-CP	[a]Pt/M48N	NaOH	H_2O	39.2%
4-CP	[a]Ru/M48N	NaOH	H_2O	0.4%
2-CP	[a]Pd/M48N(2-CP)	NaOH	H_2O	33%
3-CP	[a]Pd/M48N(3-CP)	NaOH	H_2O	65%
2,4-DCP	[b]Pd/M48N(2,4-DCP)	NaOH	H_2O	14%

Reaction conditions: catalyst (20 mg), solvent (30 mL), CPs (1 mmol), H_2 (30 mL min^{-1}), reaction time (2 h); [a] 1 mmol base, [b] 2 mmol base.

The catalytic properties of the Pd/M48N catalysts were investigated using the HDC of 4-CP as a model reaction, which has been proved to be an effective way to evaluate the removal efficiency of noble metal nano-catalysts. Contrast HDC experiments of 2-CP, 3-CP and 2,4-DCP were also tested and reaction results were exhibited in Table 2. According to the result of HDC of 4-CP in Table 2, it can be easily concluded that

the optimum condition was NaOH as base and H_2O as solvent. The HDC reaction pathway was described below: H_2 adsorbed on the active site of the M48N nano-catalyst was activated into two hydrogen atoms which combined with 4-CP also adsorbed on the surface of the M48N nano-catalyst. The C-Cl bond of 4-CP was attacked by the active hydrogen atoms to from phenol.[33] Simultaneously, in the process HDC of 4-CP, HCl was formed as by-product which can poison catalysts.[37, 38] In order to restrain the catalyst poising which caused by HCl, NaOH, Na_2CO_3, NaAc and triethyl amine were tested as base，respectively. Compared with yield value, it can be summarized that NaOH was the best choice. In the reaction process, NaCl was generated by the neutralization of HCl and NaOH. In organic solvent, low solubility of NaCl can deposits on the surface of Pd/M48N blocked the pores of M48N support, thereby inhibiting adsorption and activation which resulting in a decrease of reaction rate.[19]

According to the research of Diaz et al. size of metal NPs was an important factor on the catalytic activity. The results of the study indicated that the optimum metal size ranged from 2-4 nm. The agglomeration of smaller metal particles will cause activity reducing.[39] In addition, many studies suggested that edges and corners were the best place for support to load metal NPs in HDC.[40] Metal NPs loaded on such place can provide more surface area of active phase and exposed lattice plane can affect the selectivity of HDC. In this study, the Pd NPs possessed higher opportunity to load on the edges and corners of M48N because of unique pore structure and super-large pore

volume of M48N.

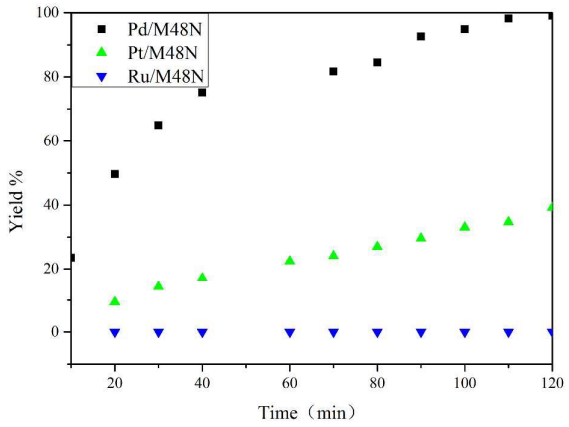

Figure 6. The yield curves of HDC of 4-CP catalyzed by Pd, Pt, Ru/M48N.

By comparing the catalytic activity of Pd/M48N, Pt/M48N and Ru/M48N, Pd/M48N showed a higher catalytic performance than Ru/M48N and Pt/M48N (Figure 6). The experimental result was in agreement with the previously reported works in which the Pd based catalysts have been found more active for HDC of 4-CP.[18, 41, 42]

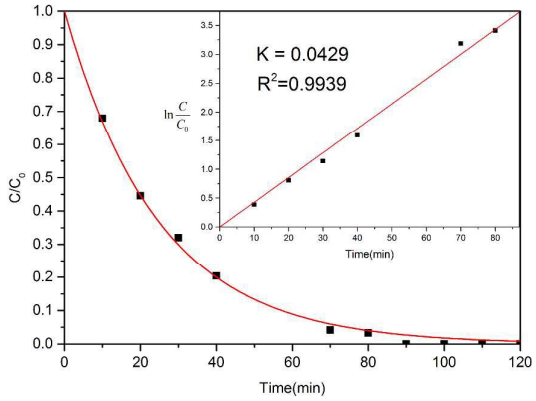

Figure 7. Fitted Kinetic Rate Constants of the HDC of 4-Chlorophenol catalyzed by Pd/M48N.

The concentration of H_2 can be considered constant since all the reactions were carried out with a high excess of that reactant. Therefore, the reaction followed pseudo-first-order reaction kinetics. According to the concentration value related to

reaction time, through plotted the logarithm of 4-CP concentration versus reaction time, the linear fittings were drew in Figure 7. The squared correlation coefficient of the line reached up to 0.9939 which indicated that the linear fittings much better conformed to first-order kinetics equations:

$$\frac{C}{C_0} = e^{-kt} \quad or \quad \ln\frac{C}{C_0} = -kt$$

The first order kinetic reaction rate constant had been calculated which was 0.0429 min^{-1}. The reaction rate constant per unit mass $k' = k/M_{Pd}$ was calculated to be 42.9 min^{-1} g^{-1}. The kinetic reaction rate of HDC catalyzed by Pd/Al_2O_3, Pd/pillared clays and Pd/KCC catalyst was 3.33 min^{-1} g^{-1}, 7.6 min^{-1} g^{-1} and 21.15 min^{-1} g^{-1}, respectively.[16, 30 32] Compared with some other Pd based catalysts which had been reported, the catalyst which Pd loaded on M48N performed higher catalytic activity. The lower catalytic activity may be due to low surface areas of Al_2O_3 with 92 m^2 g^{-1} and unordered pore structure of active carbon. This indicated the great catalytic activity of Pd/M48N nanocatalyst.

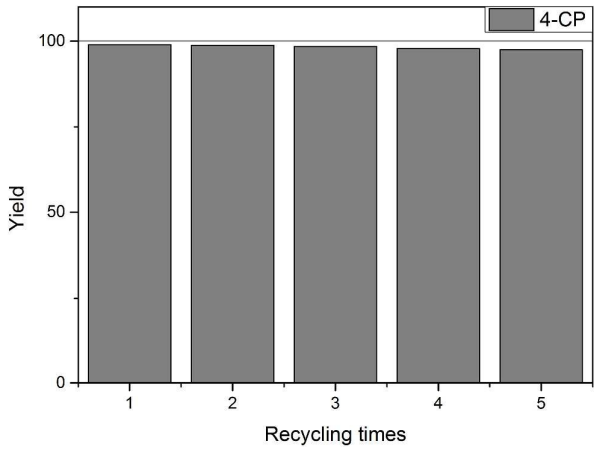

Figure 8. HDC turnover rates of 4-CP HDC over recycled catalyst.

The stability experiments is performed under optimal condition using Pd as catalyst in a centrifuge tube with H_2 supplied. The catalyst was recovered by centrifugation and simple decantation of liquid products. The catalyst was then washed with deionized water and used directly for the next cycle of the reaction without further purification. The recoverability and reusability were investigated by the HDC reaction of 4-CP and the results are summarized in Figure 8. After 5 recycling times, the metal loading of catalyst of 4.43% is measured instead of 5.01% and the catalytic activity of Pd/MSNs shows a slight weakness. This result confirmed the high rate of recyclability of the Pd/DMSNs nanocatalyst and indicated that metal loss is an influence factor for catalytic activity decreasing. In addition, by comparing TEM images (Figure 2 and Figure s1) of fresh and used catalyst there were no visible differences between the fresh and used catalyst.

4. Conclusion

Initially, M48N with ultrahigh surface areas, super-large pore volume and unique pore structure was synthesized. Pd, Pt and Ru NPs were successfully loaded on the interior surface of M48N through a method of incipient wetness impregnation. TEM, XRD, BET and XPS experiments were used for analysing M48N and as-prepared samples. Via analysing the result of hydrodechlorination reaction catalyzed by as-prepared samples, Pd/M48N showed a great catalytic performance. During 120 min reaction time, the reaction rate constant per unit mass $k' = k/M_{Pd}$ was calculated

to be 42.9 min^{-1} g^{-1} which higher than Pt, Ru/M48N and some other kind of Pd based catalysts. The good catalytic performance was due to ultrahigh surface area, super-large pore volume and unique pore structure of M48N.

References

1. A. Nair and M. K. K. Pillai, *Sci. Total Environ.*, 1992, **121**, 145-157.
2. T. T. Tetsuya Yoneda , Kenji Konuma, *J. Mol. Catal. A: Chem.*, 2007, **265**, 80–89.
3. Y. Han, W. Li, M. Zhang and K. Tao, *Chemosphere*, 2008, **72**, 53-58.
4. W. Zhang, X. Quan, J. Wang, Z. Zhang and S. Chen, *Chemosphere*, 2006, **65**, 58-64.
5. C. E. Hetrick, J. Lichtenberger and M. D. Amiridis, *Appl. Catal. B: Environ.*, 2008, **77**, 255-263.
6. M. D. Erickson, S. E. Swanson, J. D. Flora and G. D. Hinshaw, *Environ. Sci. Technol.*, 1989, **23**, 462-470.
7. E. Diaz, A. F. Mohedano, J. A. Casas, L. Calvo, M. A. Gilarranz and J. J. Rodriguez, *Appl. Catal. B: Environ.*, 2011, **106**, 469-475.
8. M. A. Keane, G. Pina and G. Tavoularis, *Appl. Catal. B: Environ.*, 2004, **48**, 275-286.
9. S. Ordonez, E. Diaz, R. F. Bueres, E. Asedegbega-Nieto and H. Sastre, *J. Catal.*, 2010, **272**, 158-168.
10. H. M. Roy, C. M. Wai, T. Yuan, J. K. Kim and W. D. Marshall, *Appl. Catal. A: Gen.*, 2004, **271**, 137-143.
11. F. D. Kopinke, K. Mackenzie, R. Koehler and A. Georgi, *Appl. Catal. A: Gen.*, 2004, **271**, 119-128.

12. L. Calvo, M. A. Gilarranz, J. A. Casas, A. F. Mohedano and J. J. Rodriguez, *Ind. Eng. Chem. Res.*, 2005, **44**, 6661-6667.

13. L. Calvo, M. A. Gilarranz, J. A. Casas, A. F. Mohedano and J. J. Rodriguez, *Appl. Catal. B: Environ.*, 2008, **78**, 259-266.

14. M. A. Lillo-Ródenas, J. Juan-Juan, D. Cazorla-Amorós and A. Linares-Solano, *Carbon*, 2004, **42**, 1371-1375.

15. G. Yuan and M. A. Keane, *Appl. Catal. B: Environ.*, 2004, **52**, 301-314.

16. E. Diaz, J. A. Casas, A. F. Mohedano, L. Calvo, M. A. Gilarranz and J. J. Rodriguez, *Ind. Eng. Chem. Res.*, 2008, **47**, 3840-3846.

17. J. Halasz, S. Meszaros and I. Hannus, *React. Kinet. Catal. Lett.*, 2006, **87**, 359-365.

18. G. Yuan and M. A. Keane, *Catal. Commun.*, 2003, **4**, 195-201.

19. M. A. Aramendia, V. Borau, I. M. Garcia, C. Jimenez, F. Lafont, A. Marinas, J. M. Marinas and F. J. Urbano, *J. Catal.*, 1999, **187**, 392-399.

20. T. Janiak and J. Okal, *Appl. Catal. B: Environ.*, 2009, **92**, 384-392.

21. J. A. Baeza, L. Calvo, M. A. Gilarranz, A. F. Mohedano, J. A. Casas and J. J. Rodriguez, *J. Catal.*, 2012, **293**, 85-93.

22. M. A. Keane, *J. Chem. Technol. Biotechnol.*, 2005, **80**, 1211-1222.

23. G. S. Pozan and I. Boz, *J. Hazard. Mater.*, 2006, **136**, 917-921.

24. G. Yuan and M. A. Keane, *Chem. Eng. Sci.*, 2003, **58**, 257-267.

25. G. Yuan and M. A. Keane, *Catal. Today*, 2003, **88**, 27-36.

26. R. F. Howe, *Appl. Catal. A: Gen.*, 2004, **271**, 3-11.

27. A. Santos, P. Yustos, A. Quintanilla, S. Rodriguez and F. Garcia-Ochoa, *Appl. Catal. B: Environ.*, 2002, **39**, 97-113.

28. P.-K. Chen, N.-C. Lai, C.-H. Ho, Y.-W. Hu, J.-F. Lee and C.-M. Yang, *Chem. Mater.*, 2013, **25**, 4269-4277.

29. E. Diaz, J. A. Casas, A. F. Mohedano, L. Calvo, M. A. Gilarranz and J. J. Rodriguez, *Ind. Eng. Chem. Res.*, 2009, **48**, 3351-3358.

30. C. B. Molina, A. H. Pizarro, J. A. Casas and J. J. Rodriguez, *Appl. Catal. B: Environ.*, 2014, **148**, 330-338.

31. L. Calvo, M. A. Gilarranz, J. A. Casas, A. F. Mohedano and J. Rodriguez, *J. Hazard. Mater.*, 2009, **161**, 842-847.

32. X. Le, Z. Dong, X. Li, W. Zhang, M. Le and J. Ma, *Catal. Commun.*, 2015, **59**, 21-25.

33. Z. Dong, X. Le, C. Dong, W. Zhang, X. Li and J. Ma, *Appl. Catal. B: Environ.*, 2015, **162**, 372-380.

34. X. Le, Z. Dong, W. Zhang, X. Li and J. Ma, *J. Mol. Catal. A: Chem.*, 2014, **395**, 58-65.

35. X. Le, Z. Dong, Y. Liu, Z. Jin, T.-D. Huy, M. Le and J. Ma, *J. Mater. Chem. A*, 2014, **2**, 19696-19706.

36. H. Deng, G. Fan and Y. Wang, *Synthesis And Reactivity In Inorganic Metal-Organic And Nano-Metal Chemistry*, 2014, **44**, 1306-1311.

37. Z. M. de Pedro, E. Diaz, A. F. Mohedano, J. A. Casas and J. J. Rodriguez, *Appl. Catal. B: Environ.*, 2011, **103**, 128-135.

38. Y. Liu, Z. Dong, X. Li, X. Le, W. Zhang and J. Ma, *RSC Advances*, 2015, **5**, 20716-20723.

39. E. Diaz, A. F. Mohedano, J. A. Casas, L. Calvo, M. A. Gilarranz and J. J. Rodriguez, *Appl. Catal. B: Environ.*, 2011, **106**, 469-475.

40. J. Xu and D. Bhattacharyya, *Ind. Eng. Chem. Res.*, 2007, **46**, 2348-2359.

41. L. Calvo, M. A. Gilarranz, J. A. Casas, A. F. Mohedano and J. J. Rodriguez, *Water Res.*, 2007, **41**, 915-923.

42. L. Calvo, M. A. Gilarranz, J. A. Casas, A. F. Mohedano and J. J. Rodriguez, *Appl. Catal. B: Environ.*, 2006, **67**, 68-76.